Received: 24 September 2024 | Revised: 25 November 2024 | Accepted: 27 November 2024

DOI: 10.1002/dad2.70059

Alzheimer's & Dementia
Diagnosis, Assessment & Disease Monitoring

RESEARCH ARTICLE

A longitudinal study of functional brain complexity in progressive Alzheimer's disease

Ru Zhang[1] | **Leon Aksman**[2] | **Dilmini Wijesinghe**[1] | **John M. Ringman**[3] | **Danny J. J. Wang**[1] | **Kay Jann**[1] | **for the Alzheimer's Disease Neuroimaging Initiative**

[1]Laboratory of Functional MRI Technology, Mark and Mary Stevens Neuroimaging and Informatics Institute, Keck School of Medicine, University of Southern California, Los Angeles, California, USA

[2]Laboratory of Neuro Imaging, Mark and Mary Stevens Neuroimaging and Informatics Institute, Keck School of Medicine, University of Southern California, Los Angeles, California, USA

[3]Memory and Aging Center, Keck School of Medicine, University of Southern California, Los Angeles, California, USA

Correspondence
Ru Zhang, Laboratory of Functional MRI Technology, Mark and Mary Stevens Neuroimaging and Informatics Institute, Keck School of Medicine, University of Southern California, 2025 Zonal Ave., Los Angeles, CA 90033, USA.
Email: ru.zhang@ini.usc.edu

Data used in preparation of this article were obtained from the Alzheimer's Disease Neuroimaging Initiative (ADNI) database. As such, the investigators within the ADNI contributed to the design and implementation of ADNI and/or provided data but did not participate in the analysis or writing of this report.

Funding information
National Institutes of Health, Grant/Award Numbers: U01 AG024904, R01AG066711, S10OD032285

Abstract

INTRODUCTION: Cross-sectional resting-state functional magnetic resonance imaging (rsfMRI) studies have revealed altered complexity with advanced Alzheimer's disease (AD) stages. The current study conducted longitudinal rsfMRI complexity analyses in AD.

METHODS: Linear mixed-effects (LME) models were implemented to evaluate altered rates of disease progression in complexity across disease groups.

RESULTS: The LME models revealed complexity of the higher frequency in the CNtoMCI group (those converted from cognitively normal [CN] to mild cognitive impairment [MCI]) decayed faster over time versus CN in the prefrontal and lateral occipital cortex; complexity of the lower frequency decayed faster in AD versus CN in various frontal and temporal regions ($p < 0.05$ & Benjamini–Hochberg corrected with $q < 0.05$).

DISCUSSION: Local functional brain activities decayed in the early stage of the disease, and long-range communications were impacted in the later stage. Our study demonstrated longitudinal changes in AD-related rsfMRI complexity, indicating its potential as an imaging biomarker of AD.

KEYWORDS
Alzheimer's disease, complexity analysis, functional magnetic resonance imaging, longitudinal study, mild cognitive impairment, resting state

Highlights

- We conducted longitudinal resting state functional magnetic resonance imaging (rsfMRI) complexity analyses using the Alzheimer's Disease Neuroimaging Initiative dataset.
- Higher-frequency complexity in the CNtoMCI group (those transitioning from cognitively normal [CN] to mild cognitive impairment [MCI]) was found to decay faster over time compared to CN, specifically in the prefrontal and lateral occipital cortex.
- Lower-frequency complexity was found to decay faster in AD versus CN in various frontal and temporal regions.
- This study demonstrated that longitudinal changes in rsfMRI complexity could serve as a potential imaging biomarker for Alzheimer's disease.

1 | BACKGROUND

Alzheimer's disease (AD) is a progressive, irreversible neurodegenerative disorder characterized by cognitive decline, memory impairment, and functional deterioration. Millions of Americans currently suffer from AD and this number could increase to 13.8 million by 2050.[1] Mild cognitive impairment (MCI) is considered a transitional stage between normal aging and dementia. Individuals with MCI tend to progress to probable AD at a rate of ≈ 10% to 15% per year.[2] The pathophysiological changes in AD include the accumulation of toxic species of amyloid beta (Aβ) and the development of neurofibrillary tangles of hyperphosphorylated tau protein.[3] Possession of the ε4 allele of apolipoprotein E (*APOE*) is the primary genetic risk factor for late-onset AD.[4]

Functional connectivity (FC), which refers to the statistical association between the neural signals of different brain regions, has emerged as a valuable tool in understanding the altered brain networks and functions associated with AD.[5–8] Non-linear statistical approaches, which complement the measure of FC, have been used to inspect the functional brain complexity alteration in AD pathology.[9–20] Complexity in this context refers to the variability and unpredictability of brain signal patterns. High complexity is associated with a functional brain system capable of adapting to various cognitive demands. Conversely, a reduction in complexity suggests a decline in the system's adaptive capabilities, which is characteristic of neurodegenerative diseases like AD.

Sample entropy (SampEn) and multiscale entropy (MSE) have been used to measure complexity in time series.[21] SampEn is the negative logarithm of the conditional probability that subseries of length m within a time series of length N that match pointwise within a tolerance r will also match at the next point, where self-matches are excluded. "Coarse-grained" time series of lengths $N/1$, $N/2$, …, and N/a can be formed through averaging consecutive data points. SampEn is calculated based on each of the temporal scales (i.e., scales 1 to a). MSE stands for SampEn across multiple temporal scales. Studies have shown that MSE at high frequencies (low scale numbers) may represent the complexity of local neuronal processes, while MSE at low frequencies (high scale numbers) reflect the complexity of input from distributed, long-range communications, offering insights into both localized and global brain functions.[22]

Previous resting-state functional magnetic resonance imaging (rsfMRI) complexity studies in AD have predominantly revealed monotonically declining complexity from cognitively normal (CN) to MCI to AD.[10,11,13,20] However, one study showed SampEn slightly increased from CN to early MCI, but quickly dropped to be below SampEn of controls in late MCI, and fell further in AD.[12] Notably, these studies relied on cross-sectional cohorts. We performed a longitudinal analysis of rsfMRI complexity to investigate AD-related functional brain changes over time. SampEn and MSE in different groups of patients is the most commonly reported complexity metric in AD literature and has repeatedly been demonstrated to distinguish between different stages of AD. While other complexity metrics are available, using SampEn and MSE in our study, for the first time in investigating longitudinal changes, remains directly comparable to current literature. We formed three pathology stable groups (i.e., groups of CN, MCI, and AD) and two conversion groups (Group CNtoMCI: those converted from CN to MCI; Group MCItoAD: those converted from MCI to AD). We hypothesized that (1) the complexity of the five diagnostic groups was ordered monotonically as CN ≥ CNtoMCI ≥ MCI ≥ MCItoAD ≥ AD and (2) complexity in the CNtoMCI, MCI, MCItoAD, and AD groups decayed faster over time than in the CN group.

2 | METHODS

2.1 | Demographic, clinical, and imaging data

Data used in the preparation of this article were obtained from the Alzheimer's Disease Neuroimaging Initiative (ADNI) database. For the current study, we used demographic, clinical, T1 structural, and rsfMRI data from ADNI. The rsfMRI imaging data were obtained by using an echo-planar imaging (EPI) sequence with an acquisition time of 7 to 10 minutes (repetition time = 3000 ms, echo time = 30 ms, flip angle = 80°, matrix = 64 × 64, number of slices = 48). More information about the scanners can be found in Table S1 in supporting information.

The selected sample included five diagnostic groups, comprising a total of 349 subjects and a total of 911 rsfMRI scans. The CN group consisted of those who remained CN at every visit. The CNtoMCI group included subjects who converted from CN to MCI. The MCI group consisted of those who remained MCI once they were diagnosed as MCI. The MCItoAD group included subjects who converted from MCI to AD. The AD group consisted of those who remained AD once they were diagnosed with AD.

Each subject had at least two rsfMRI scans from different visits, and the scans with excessive motion (framewise displacement > 0.20 mm) were excluded. For the CNtoMCI group, we required each subject to have at least one scan while they were CN and at least one scan while they were diagnosed as MCI. For the MCItoAD group, we required each subject to have at least one scan while they were diagnosed as MCI and at least one scan while they were diagnosed as AD. Table 1 displays the demographic information for each subject group. The five groups matched in terms of education years but differed in sex, age of the first rsfMRI scan, and framewise displacement ($p < 0.05$).

2.2 | Data preprocessing and fMRI complexity analysis

Preprocessing was performed using the CONN toolbox[23] and included motion realignment, correction for motion artifacts, and co-registration to the corresponding anatomical image. The anatomical images underwent tissue segmentation and were normalized to the Montreal Neurological Institute (MNI) stereotaxic space. Functional images were then normalized based on structural data, resampled to $2 \times 2 \times 2$ mm^3 voxel size, and spatially smoothed with a 6 mm full width at half-maximum (FWHM) 3D isotropic Gaussian kernel.

Complexity analysis was conducted with the LOFT Complexity Toolbox. Voxel-wise SampEn with pattern length $m = 2$ and sensitivity threshold $r = 0.3$ was computed for temporal scales $a = 1$ to 4 (0.33–0.08 Hz, see the mathematical definition of SampEn in the supporting information). The choice of m and r was based on the recommendation by Roediger et al.,[24] who identified this as the optimal combination for computing SampEn for rsfMRI time series in the cortical regions. While different values for m and r may also be effective,[25] the current choice struck a balance between capturing short-term signal dynamics and ensuring robust estimation across subjects. The area under the curve for SampEn across scales 1 to 4, termed aucMSE, was also computed. Fourteen meta regions of interest (meta-ROIs) were formed from the Harvard–Oxford atlas,[26] that is, the prefrontal, insula, superior frontal, middle frontal, inferior frontal, cingulate, precentral, precuneus, temporal pole, lateral temporal, medial temporal, lateral parietal, lateral occipital, and medial occipital. Finally, mean aucMSE and mean SampEn at each temporal scale within each meta-ROI were calculated.

RESEARCH IN CONTEXT

1. **Systematic review**: Previous cross-sectional studies using resting-state functional magnetic resonance imaging (rsfMRI) have shown altered brain complexity in Alzheimer's disease (AD), but longitudinal changes remain unclear.
2. **Interpretation**: This study applied longitudinal linear mixed-effects models to rsfMRI data from the Alzheimer's Disease Neuroimaging Initiative (ADNI). Individuals transitioning from cognitively normal (CN) to mild cognitive impairment (MCI) showed a faster decline in higher-frequency complexity in the prefrontal and lateral occipital regions compared to stable CN individuals. In the AD group, lower-frequency complexity decayed more rapidly in the frontal and temporal regions, consistent with previous cross-sectional findings. These results suggest that early AD disrupts local brain activity, while long-range communication breakdowns occur in later stages.
3. **Future directions**: Future studies should validate these rsfMRI complexity changes as biomarkers in diverse populations, potentially integrating other neuroimaging and cognitive measures for personalized treatment strategies.

2.3 | Statistical analysis

2.3.1 | Main analyses

Six linear mixed-effects (LME) models were developed to evaluate the main effects of group and group-by-time (time is short for time since the first rsfMRI scan) interactions for mean aucMSE of the whole gray matter (Model 1), mean aucMSE for each meta-ROI (Model 2), and mean SampEn for each meta-ROI (Models 3–6 for temporal scale $a = 1$ to 4, respectively). Sex, education (in years), scanner type, number of fMRI volumes, and framewise displacement were included as covariates. There were two baseline covariates in each model, that is, age of the first rsfMRI scan and mean entropy of the whole gray matter of the first rsfMRI scan, to account for the historical or social factors that have shaped each subject's functional brain before their first rsfMRI scan.

For the main effects of group, we were interested in the paired comparisons for any two groups among the five groups (i.e., CN, CNtoMCI, MCI, MCItoAD, and AD). For the group-by-time interactions, we were interested in the changing rate in complexity over time in any group (i.e., CNtoMCI or MCI or MCItoAD or AD) against CN. Benjamini–Hochberg (BH) correction[27] was performed to evaluate the

TABLE 1 Information of the five diagnostic groups.

	CN ($N = 156$)	CNtoMCI ($N = 16$)	MCI ($N = 80$)	MCItoAD ($N = 20$)	AD ($N = 23$)	Group comparison	
						Statistic	*p* value
Number of rsfMRI scans per subject	2.827 ± 1.125	3.625 ± 1.708	3.363 ± 1.204	4.250 ± 2.245	2.652 ± 0.885	$F = 8.159$	0.000*
Sex (F/M)	93/63	9/7	33/47	11/9	9/14	$\chi^2 = 31.343$	0.000*
Age of the first rsfMRI scan	72.224 ± 6.669	76.027 ± 7.057	74.252 ± 8.027	73.296 ± 7.943	76.315 ± 8.360	$F = 2.716$	0.030*
Education of years	16.641 ± 2.410	16.875 ± 2.604	16.363 ± 2.874	16.000 ± 2.128	15.522 ± 3.043	$F = 21.287$	0.275
Framewise displacement (mm)	0.112 ± 0.042	0.111 ± 0.041	0.119 ± 0.040	0.122 ± 0.043	0.136 ± 0.036	$F = 5.845$	0.000*

Note: Key to Table 1: $^*p < 0.05$.
Abbreviations: AD, Alzheimer's disease; CN, cognitively normal; MCI, mild cognitive impairment; rsfMRI, resting state functional magnetic resonance imaging.

significance of all the effects.

$$\begin{aligned}&\text{Mean aucMSE of the whole gray matter}\\&= \beta_0 + \beta_1\,\text{Group} + \beta_2\,\text{Time since the 1st rsfMRI scan} + \beta_3\,\text{Group}\\&\times \text{Time since the 1st rsfMRI scan}\\&+ \beta_4\,\text{Sex} + \beta_5\,\text{Education} + \beta_6\,\text{Number of volumes per rsfMRI scan}\\&+ \beta_7\,\text{Scanner} + \beta_8\,\text{Mean aucMSE of the whole gray matter of the}\\&\quad\text{1st rsfMRI scan}\\&+ \beta_9\,\text{Age of the 1st rsfMRI scan} + \beta_{10}\text{Framewise displacement}\\&+ (1 + \text{Time since the 1st rsfMRI scan}|\text{Subject})\,.\end{aligned} \tag{1}$$

$$\begin{aligned}&\text{Mean aucMSE for each meta} - \text{ROI}\\&= \beta_0 + \beta_1\,\text{Group} + \beta_2\,\text{Time since the 1st rsfMRI scan} + \beta_3\,\text{Group}\\&\times \text{Time since the 1st rsfMRI scan}\\&+ \beta_4\,\text{Sex} + \beta_5\,\text{Education} + \beta_6\,\text{Number of volumes per rsfMRI scan}\\&+ \beta_7\,\text{Scanner} + \beta_8\,\text{Mean aucMSE of the whole gray matter of the}\\&\quad\text{1st rsfMRI scan}\\&+ \beta_9\,\text{Age of the 1st rsfMRI scan} + \beta_{10}\text{Framewise displacement}\\&+ (1 + \text{Time since the 1st rsfMRI scan}|\text{Subject})\,.\end{aligned} \tag{2}$$

$$\begin{aligned}&\text{Mean SampEn for each meta} - \text{ROI}\\&= \beta_0 + \beta_1\,\text{Group} + \beta_2\,\text{Time since the 1st rsfMRI scan} + \beta_3\,\text{Group}\\&\times \text{Time since the 1st rsfMRI scan}\\&+ \beta_4\,\text{Sex} + \beta_5\,\text{Education} + \beta_6\,\text{Number of volumes per rsfMRI scan}\\&+ \beta_7\,\text{Scanner} + \beta_8\,\text{Mean SampEn of the whole gray matter of the}\\&\quad\text{1st rsfMRI scan}\\&+ \beta_9\,\text{Age of the 1st rsfMRI scan} + \beta_{10}\text{Framewise displacement}\\&+ (1 + \text{Time since the 1st rsfMRI scan}|\text{Subject})\,.\end{aligned} \tag{3–6}$$

2.3.2 | Secondary analyses

In the CN group, we investigated the association between complexity and time since the first rsfMRI scan and the association between complexity and age of the first rsfMRI scan (see Model I1–I6 in the supporting information).

We assessed the amyloid status for each subject where amyloid positron emission tomography (PET) standardized uptake value ratio (SUVR) > 1.11 indicates amyloid positive (A+) whereas SUVR < 1.11 indicates amyloid negative (A–). Individuals with A+ labeling are considered on the AD progression spectrum.[28] First, the whole sample was divided into two groups A+ and A– (see Table S2 in supporting information), and evaluated for the main effects of amyloid status and the amyloid status-by-time interactions (see Model II1–II6 in the supporting information). Second, four subgroups of adequate sample sizes (n in each group ≥ 14) were extracted from the stable CN subjects and the stable MCI subjects, denoted as A–&CN, A+&CN, A–&MCI, and A+&MCI (see Table S3) and evaluated for the interaction between amyloid status (A+ vs. A–) and clinical diagnosis (CN vs. MCI) on complexity and on the change of complexity over time (see Model III1–III6 in the supporting information).

APOE status is associated with increased Aβ deposition across the AD spectrum and with increased tau protein and cognitive decline in the prodromal AD stage, thereby increasing the risk of AD.[29] First, the whole sample was divided into three groups (*APOE* ε4–, *APOE* ε4+, and *APOE* ε4++) regardless of the clinical diagnosis (Table S4 in supporting information) and assessed for main effects of *APOE* status and the *APOE* status-by-time interactions (see Model IV1–IV6 in the supporting information). Second, four subgroups of adequate sample sizes (n in each group ≥ 14) were formed from the original CN and MCI groups, denoted as *APOE* ε4–&CN, *APOE* ε4+&CN, *APOE* ε4–&MCI, and *APOE* ε4+&MCI (see Table S5 in supporting information) and assessed for the interaction between *APOE* status (*APOE* ε4– vs. *APOE* ε4+) and clinical diagnosis (CN vs. MCI) on complexity and on the change of complexity over time (see Model V1–V6 in the supporting information).

3 | RESULTS

3.1 | Main analyses

Model 1 revealed no significant main effect of group; however, aucMSE of the whole gray matter in AD decayed faster than CN

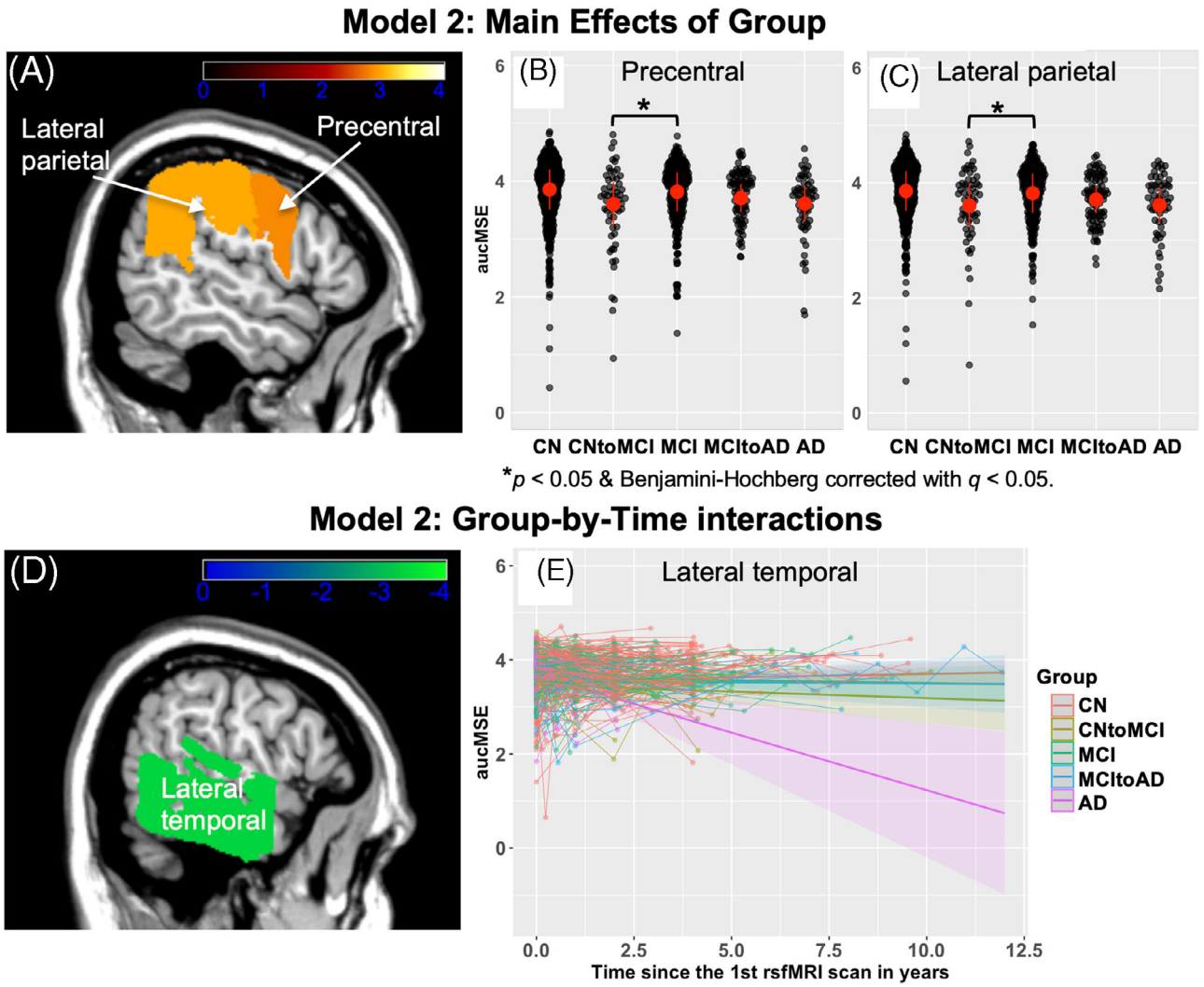

FIGURE 1 Significant main effects of group and group-by-time interactions obtained from Model 2 for ($p < 0.05$ & BH corrected with $q < 0.05$): (A) t values of the main effects of group in the precentral and lateral parietal, (B) observed (black dots) and predicted aucMSE (red dots and line segments) in each group in the precentral, (C) observed (black dots) and predicted aucMSE (red dots and line segments) in each group in the lateral parietal, (D) t value of the group-by-time interaction in the lateral temporal, and (E) observed (spaghetti plots) and predicted (solid lines and shadows) aucMSE over time in each group in the lateral temporal. AD, Alzheimer's disease; aucMSE, area under the curve for sample entropy; BH, Benjamini–Hochberg; CN, cognitively normal; MCI, mild cognitive impairment; rsfMRI, resting state functional magnetic resonance imaging.

over time ($p < 0.05$). Model 2 revealed aucMSE of MCI was significantly greater than CNtoMCI in the precentral and lateral parietal cortices; AucMSE of AD decayed faster than CN over time in the lateral temporal cortex (Figure 1; $p < 0.05$ & BH corrected with $q < 0.05$). Models 3–6 revealed SampEn of MCI at scales 1, 2, and 3 was significantly greater than CNtoMCI in the precentral and lateral parietal cortices, and SampEn of MCItoAD at scale 2 was significantly lower than MCI in the lateral occipital cortex. At scale 1, CNtoMCI decayed faster over time than CN in the prefrontal and lateral occipital cortices. At scale 2 to 4, AD decayed faster than CN in various frontal and temporal regions (Table 2, Figure 2 and Figure 3; $p < 0.05$ & BH corrected with $q < 0.05$).

3.2 | Secondary analyses

3.2.1 | Healthy aging

We found no significant longitudinal change in complexity as there was no significant association between complexity and time since the first rsfMRI scan in Model I1 to I6. However, we found a general effect of age in the medial occipital cortex as significant negative associations were found between complexity and age of the first rsfMRI scan (ranged from 56 to 91 years old) for aucMSE and SampEn at scales 3 and 4 in this region (coefficient = −0.009, −0.004, and −0.005, $t = -2.954, -3.329$, and -3.960, respectively, $p < 0.05$ & BH corrected with $q < 0.05$).

TABLE 2 The significant results obtained from Models 3–6.

SampEn	Main effect of group	Group-by-time interaction
Scale 1 (0.33 HZ)	CNtoMCI < MCI in the precentral and lateral parietal	CNtoMCI decayed faster than CN in the prefrontal and lateral occipital
Scale 2 (0.17 HZ)	CNtoMCI < MCI in the precentral and lateral parietal; MCItoAD < MCI in the lateral occipital	AD decayed faster than CN in the lateral temporal
Scale 3 (0.11 HZ)	CNtoMCI < MCI in the precentral and lateral parietal	AD decayed faster than CN in the prefrontal, middle frontal, inferior frontal, lateral temporal, and medial temporal
Scale 4 (0.08 HZ)	None	AD decayed faster than CN in the prefrontal, lateral temporal, and medial temporal

Note: Key to Table 2: All the results displayed were based on $p < 0.05$ & BH correction with $q < 0.05$.
Abbreviations: AD, Alzheimer's disease; BH, Benjamini–Hochberg; CN, cognitively normal; MCI, mild cognitive impairment.

3.2.2 | Effects related to amyloid status and association with clinical diagnosis

No significant main effect of amyloid status was found, nor were there any significant interactions between amyloid status and time. However, we found a significant amyloid status-by-group-by-time interaction in the temporal pole for SampEn at scale 3 ($p < 0.05$ & BH corrected with $q < 0.05$). Within CN, the change of complexity over time was not significantly different between different amyloid statuses. However, within MCI the complexity of A− decayed significantly more quickly over time than A+ (Figure 4). For those who had amyloid PET data in at least two visits, the changes of SUVR in the A−&CN, A+&CN, A−&MCI, and A+&MCI groups were not significantly different ($F = 3.658$, $p > 0.05$; for the spaghetti plot of SUVR over time, please see Figure S1 in supporting information). It indicated that the observed significant amyloid status-by-group-by-time interaction did not seem to result from different amounts of longitudinal change in amyloid load in the four groups.

3.2.3 | Effects related to *APOE* status and association with clinical diagnosis

No significant main effect of *APOE* status was found, nor were there any significant interactions between *APOE* status and time. No significant interaction between *APOE* status (*APOE* ε4− vs. *APOE* ε4+) and group (CN vs. MCI) was found, nor were any significant *APOE* status-by-group-by-time interactions.

4 | DISCUSSION

The main findings of the current study were the MCI group had significantly higher aucMSE and SampEn at scales 1, 2, and 3 in the precentral and lateral parietal cortices compared to the CNtoMCI group, and also significantly higher SampEn at scale 2 in the lateral occipital cortex compared to the MCItoAD group. The second main finding was that gray matter aucMSE showed a faster decay over time in the AD group than in the CN group, specifically in the lateral temporal cortex. While aucMSE reflects general changes in complexity, SampEn appears to reflect more detailed longitudinal regional changes of complexity. Low scales (i.e., high temporal frequencies) represent local functional brain changes, in this study observed predominantly as the decay of complexity in the prefrontal and lateral occipital in the early stage of the disease, whereas high scales (i.e., low temporal frequencies) are thought to reflect integration of long-range communications within brain areas, which we found to decay in the frontal and temporal regions in the later stage of the disease.

We hypothesized that rsfMRI complexity would continuously decrease with the severity of the disease. However, our data revealed that the MCI group exhibited higher complexity than the CNtoMCI and MCItoAD groups. The affected regions included the precentral, lateral parietal, and lateral occipital cortices. This inverted U shape pattern has been observed previously[12] and could suggest some compensatory mechanism in the early disease stage. Brain reserve refers to the brain's ability to tolerate pathological damage while maintaining cognitive function.[30] In this study, the MCI group exhibited higher complexity than those with milder symptoms (CNtoMCI), which suggested an attempt to preserve cognitive ability through elevated effort. The MCItoAD group showed lower complexity than the MCI group, indicating the exhaustion of brain reserve, impaired function, and thus leading to the onset of dementia. The inverted U shape pattern was also reported in the same regions using other modalities. Vannini et al.[30] observed increased activation in the superior parietal lobe in MCI compared to the healthy elder controls in an angle discrimination fMRI task. Prvulovic et al.[31] used the same task and found reduced activation in the same region in the AD subjects. Terry et al.'s[32] meta-analysis of 14 task -fMRI studies revealed greater activation in the precentral gyrus and inferior occipital gyrus in the MCI compared to the healthy elder adults. By contrast, no clusters showed increased activity for the AD group than the control group.

Additionally, we found that within the MCI group, the complexity of the A− subjects decayed more quickly over time than that of the A+ subjects in the temporal pole. It might indicate that A+&MCI subjects must increasingly compensate over time to achieve a cognitive level comparable to A−&MCI subjects. This further suggested that brain reserve in the A+&MCI subjects might be the primary factor contributing to the inverted U–shape pattern observed in the main

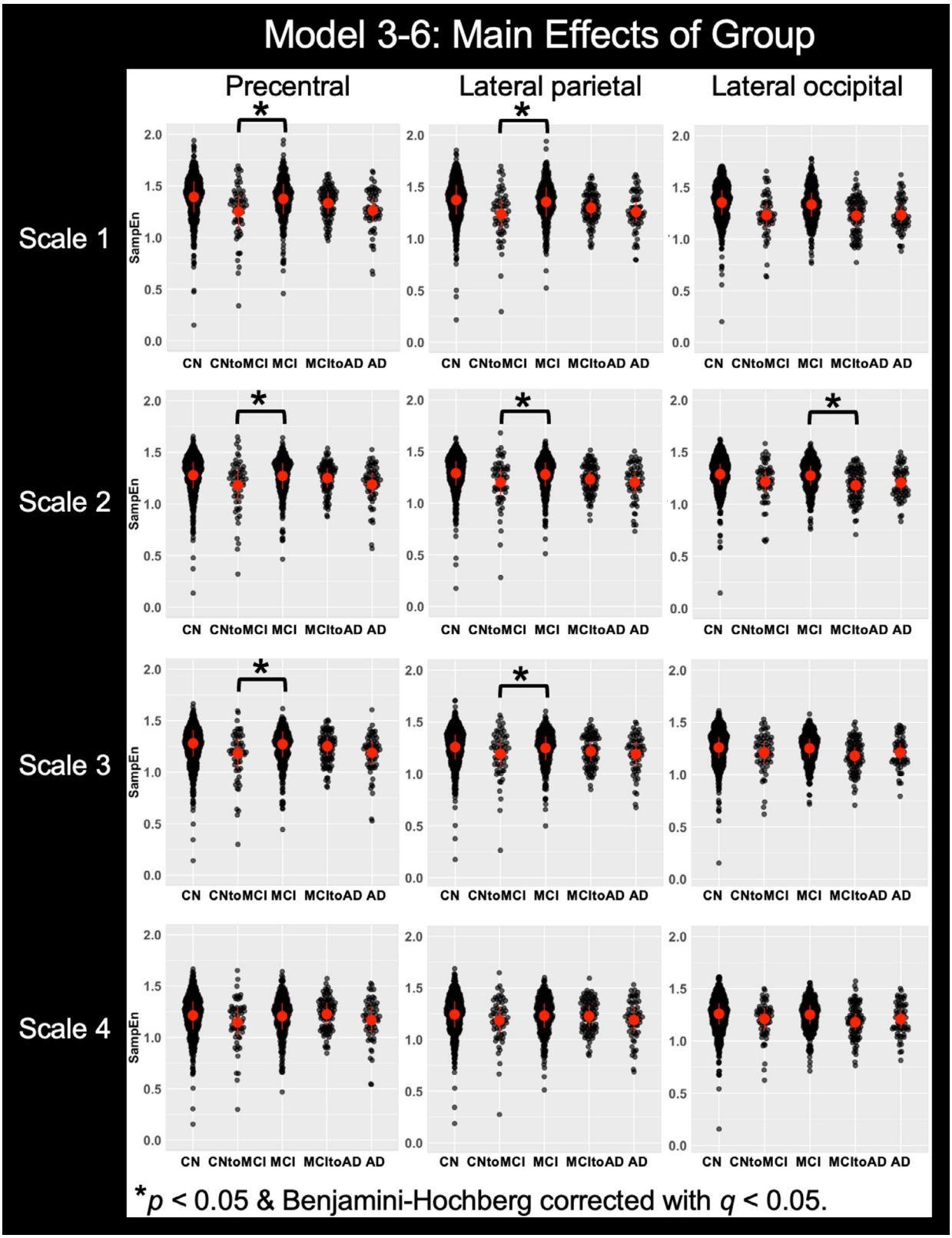

FIGURE 2 Significant main effects of group obtained from Models 3–6 ($p < 0.05$ & BH corrected with $q < 0.05$). Observed (black dots) and predicted SampEn (red dots and line segments) are displayed for each scale in each group in the precentral, lateral parietal, and lateral occipital. AD, Alzheimer's disease; BH, Benjamini–Hochberg; CN, cognitively normal; MCI, mild cognitive impairment; SampEn, sample entropy.

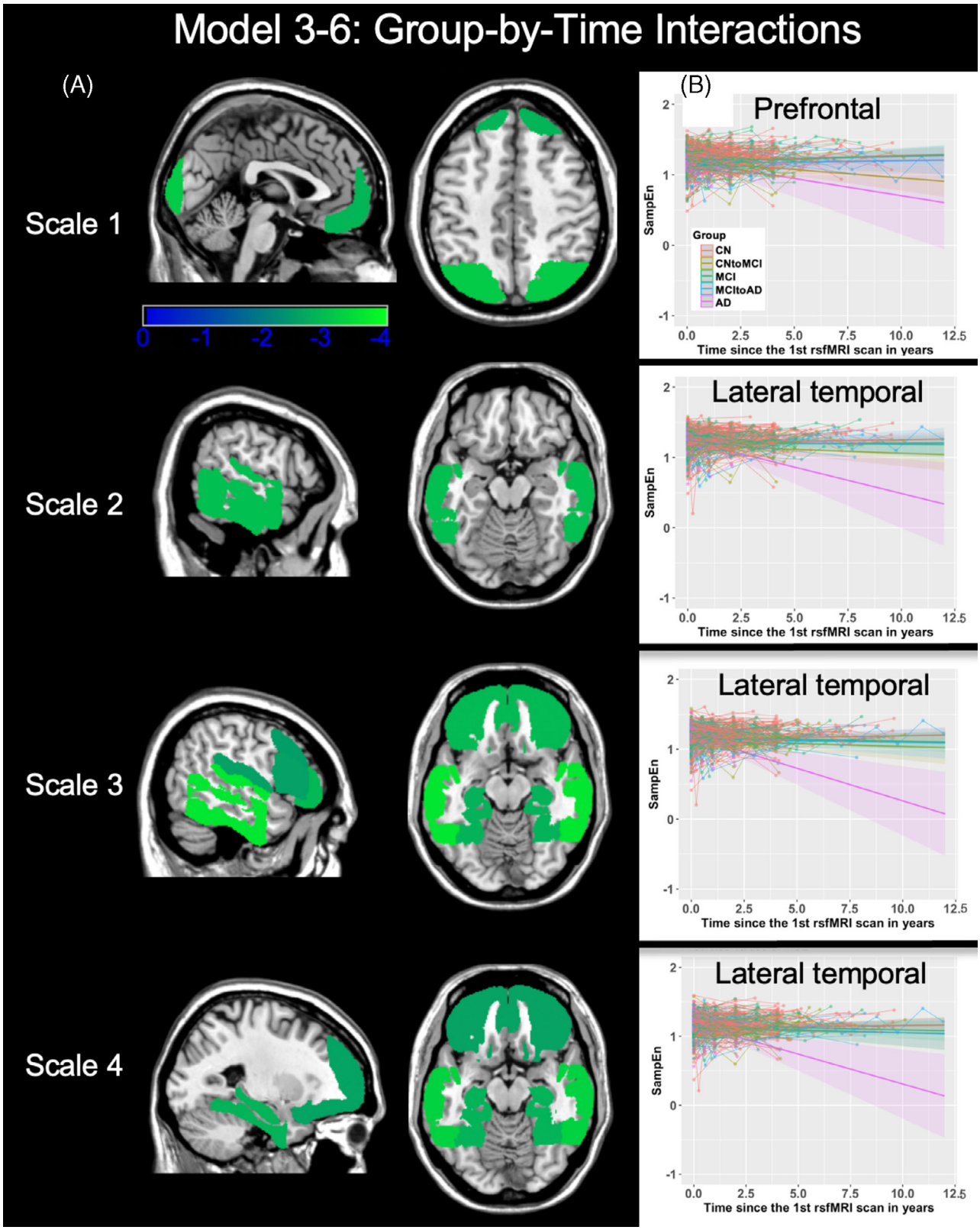

FIGURE 3 Significant group-by-time interactions obtained from Models 3–6 ($p < 0.05$ & BH corrected with $q < 0.05$). (A) t values for all the regions that showed significant group-by-time interactions on SampEn for each scale. (B) Observed (spaghetti plots) and predicted (solid lines and shadows) SampEn over time in each group in the prefrontal at scale 1 and in the lateral temporal at scale 2, 3, and 4. AD, Alzheimer's disease; aucMSE, area under the curve for sample entropy; BH, Benjamini–Hochberg; CN, cognitively normal; MCI, mild cognitive impairment; rsfMRI, resting state functional magnetic resonance imaging; SampEn, sample entropy.

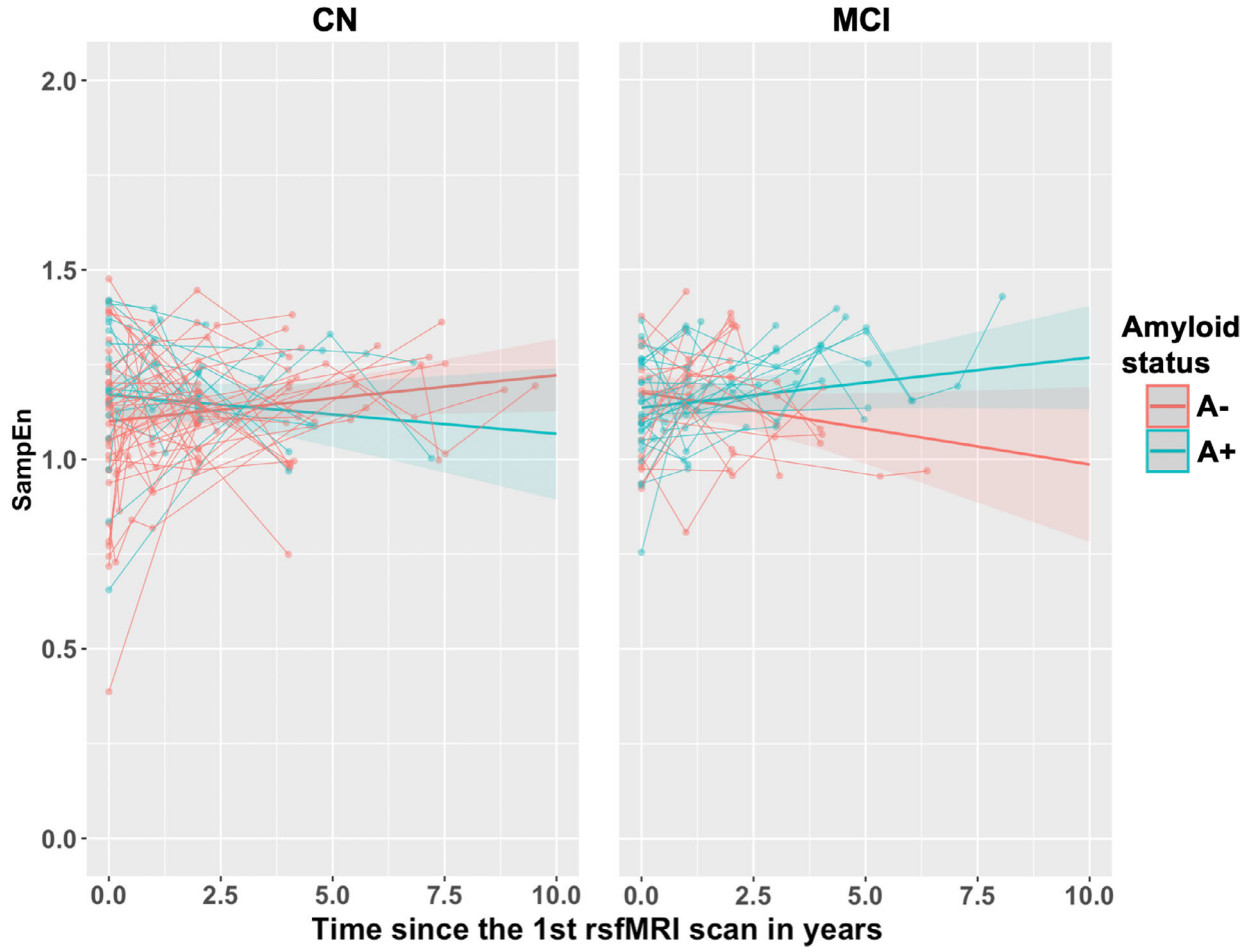

FIGURE 4 A significant amyloid status-by-group-by-time interaction was observed in the temporal pole from Model II5 (i.e., SampEn at scale 3; $p < 0.05$ & BH corrected with $q < 0.05$). Observed (spaghetti plots) and predicted (solid lines and shadows) complexity over time is displayed. BH, Benjamini–Hochberg; CN, cognitively normal; MCI, mild cognitive impairment; rsfMRI, resting state functional magnetic resonance imaging; SampEn, sample entropy.

analysis. This observation also highlighted the importance of including biological markers with clinical diagnosis in longitudinal studies on functional brain alteration of AD pathology. Recent longitudinal studies in FC supported this notion by showing that the change rate of FC in MCI was significantly different in the high-amyloid individuals than the low-amyloid individuals.[33,34]

We also found gray matter aucMSE showed a faster decay over time in the AD group than in the CN group, specifically in the lateral temporal cortex, which aligned with the primary hypothesis, and the detailed regional longitudinal changes were reflected by analyses on SampEn at different scales. Our observation showed that in the early stages of AD progression, there was a marked longitudinal decay of high-frequency SampEn, representing local functional brain activities[22] in the prefrontal and lateral occipital regions. This early involvement was consistent with the role of the prefrontal cortex in executive functions and the lateral occipital cortex in visual processing, both of which could be affected in the initial phases of AD.[35,36] With the advanced disease stage, there was a notable impact on the processing of long-range communications within the brain (low-frequency SampEn), with the frontal and temporal regions being particularly affected in the current AD sample. Sun et al.[37] reviewed studies on complexity in MCI and AD using fMRI, electroencephalography, and magnetoencephalography. They found AD patients showed reduced signal complexity in the frontal and temporal cortices compared to healthy individuals, supporting the current findings.

In terms of healthy aging, significant negative associations were found between complexity and age of the first rsfMRI scan for aucMSE and SampEn at scales 3 and 4 in the medial occipital cortex, while longitudinal changes over up to 10 years were not significant. The relationship between rsfMRI complexity and age in healthy elders has been inconsistent in the literature, with all studies being cross-sectional.[12,38–40] Longitudinal studies over a longer period are needed to clarify how complexity changes with healthy aging.

Several caveats should be considered for the current results. First, in the current study, we used SampEn and aucMSE to measure the irregularity and unpredictability of the rsfMRI time series. These metrics are particularly effective in capturing short-term changes in signal complexity. Other complexity measures like the fractal dimension and Hurst exponent assess the global structure and long-term memory of time series data. However, similar analyses using

alternative complexity measures can be conducted, and we expect they potentially yield significant findings regarding the main effects of group and group-by-time interactions. Second, a power analysis was conducted to estimate the sample size needed for each group in the LME model. Please find the details in the supporting information and Figure S2 in supporting information. A sample size ≥ 14 is needed for 80% power. Accordingly, to investigate the interactions between *APOE* status and clinical diagnosis, the whole sample should be divided into 3 by 5 groups, representing three levels of *APOE* status and five levels of diagnostic groups. Our sample supported only 2 by 2 groups from the CN and MCI groups, each with two *APOE* levels (*APOE* ε4− vs. *APOE* ε4+). The same limitation occurred for the interactions between amyloid status and clinical diagnosis. Third, in addition to amyloid, the role of tau in AD is well known, but we found insufficient data on tau PET and even more limited data on p-tau (phosphorylated tau) levels in cerebrospinal fluid in the ADNI database. Investigation of longitudinal change of complexity associated with tau or related to the interactions between tau status and clinical diagnosis was not possible but holds promise for future studies as ADNI continues to gather more data. Recently, we[13,41] reported significant associations between tau deposition and MSE in the medial temporal lobe and precuneus but not between amyloid and MSE, indicating tau is a better predictor for cognitive decay in AD than amyloid. Finally, we did not include regional amyloid PET SUVR as a covariate in Model II1–II6 and Model III1–III6 as there were too many missing data points for the current longitudinal sample because amyloid PET and rsfMRI scans were not always acquired at the same visit.

In summary, our study using, for the first time, longitudinal data to investigate changes in rsfMRI complexity demonstrates it offers a novel, alternative method for detecting and monitoring the progression of AD specifically in light of cognitive decline and potentially to differentiate subgroups with and without brain reserve. Consequently, rsfMRI complexity holds promise as a non-invasive, reliable biomarker that could enhance our understanding of AD and improve patient outcomes.

ACKNOWLEDGMENTS

Data collection and sharing for this project was funded by the Alzheimer's Disease Neuroimaging Initiative (ADNI) (National Institutes of Health Grant U01 AG024904) and DOD ADNI (Department of Defense award number W81XWH-12-2-0012). ADNI is funded by the National Institute on Aging, the National Institute of Biomedical Imaging and Bioengineering, and through generous contributions from the following: AbbVie, Alzheimer's Association; Alzheimer's Drug Discovery Foundation; Araclon Biotech; BioClinica, Inc.; Biogen; Bristol-Myers Squibb Company; CereSpir, Inc.; Cogstate; Eisai Inc.; Elan Pharmaceuticals, Inc.; Eli Lilly and Company; EuroImmun; F. Hoffmann-La Roche Ltd and its affiliated company Genentech, Inc.; Fujirebio; GE Healthcare; IXICO Ltd.; Janssen Alzheimer Immunotherapy Research & Development, LLC.; Johnson & Johnson Pharmaceutical Research & Development LLC.; Lumosity; Lundbeck; Merck & Co., Inc.; Meso Scale Diagnostics, LLC.; NeuroRx Research; Neurotrack Technologies; Novartis Pharmaceuticals Corporation; Pfizer Inc.; Piramal Imaging; Servier; Takeda Pharmaceutical Company; and Transition Therapeutics. The Canadian Institutes of Health Research is providing funds to support ADNI clinical sites in Canada. Private sector contributions are facilitated by the Foundation for the National Institutes of Health (http://www.fnih.org). The grantee organization is the Northern California Institute for Research and Education, and the study is coordinated by the Alzheimer's Therapeutic Research Institute at the University of Southern California. ADNI data are disseminated by the Laboratory for Neuro Imaging at the University of Southern California.

This project was funded by NIH R01AG066711 and S10OD032285. The content is solely the responsibility of the authors and does not necessarily represent the official views of the National Institutes of Health.

CONFLICT OF INTEREST STATEMENT

The authors declare no conflicts of interest. Author disclosures are available in the supporting information.

CONSENT STATEMENT

All participants in the ADNI study provided informed consent, which allows their data to be shared with qualified researchers. The data we are accessing and analyzing in this study have been de-identified to ensure that no personally identifiable information (PII) is included. The use of ADNI data strictly adheres to the ethical guidelines established by ADNI, and we are committed to maintaining the confidentiality and security of this data.

REFERENCES

1. Hebert LE, Weuve J, Scherr PA, Evans DA. Alzheimer disease in the United States (2010-2050) estimated using the 2010 census. *Neurology*. 2013;80(19):1778-1783. doi:10.1212/WNL.0b013e31828726f5
2. Grundman M, Petersen RC, Ferris SH, et al. Mild cognitive impairment can be distinguished from Alzheimer disease and normal aging for clinical trials. *Arch Neurol*. 2004;61(1):59-66. doi:10.1001/archneur.61.1.59
3. Leoni V. The effect of apolipoprotein E (ApoE) genotype on biomarkers of amyloidogenesis, tau pathology and neurodegeneration in Alzheimer's disease. *Clin Chem Lab Med*. 2011;49(3):375-383. doi:10.1515/CCLM.2011.088
4. Emrani S, Arain HA, DeMarshall C, Nuriel T. APOE4 is associated with cognitive and pathological heterogeneity in patients with Alzheimer's disease: a systematic review. *Alzheimers Res Ther*. 2020;12(1):141. doi:10.1186/s13195-020-00712-4
5. Ibrahim B, Suppiah S, Ibrahim N, et al. Diagnostic power of resting-state fMRI for detection of network connectivity in Alzheimer's disease and mild cognitive impairment: a systematic review. *Hum Brain Mapp*. 2021;42(9):2941-2968. doi:10.1002/hbm.25369
6. Sheline YI, Raichle ME. Resting state functional connectivity in preclinical Alzheimer's disease. *Biol Psychiatry*. 2013;74(5):340-347. doi:10.1016/j.biopsych.2012.11.028
7. Eyler LT, Elman JA, Hatton SN, et al. Resting state abnormalities of the default mode network in mild cognitive impairment: a systematic review and meta-analysis. *J Alzheimers Dis*. 2019;70(1):107-120. doi:10.3233/JAD-180847
8. Badhwar A, Tam A, Dansereau C, Orban P, Hoffstaedter F, Bellec P. Resting-state network dysfunction in Alzheimer's disease: a systematic review and meta-analysis. *Alzheimers Dement (Amst)*. 2017;8:73-85. doi:10.1016/j.dadm.2017.03.007
9. Xue SW, Guo Y, AsDN Initiative. Increased resting-state brain entropy in Alzheimer's disease. *Neuroreport*. 2018;29(4):286-290. doi:10.1097/WNR.0000000000000942

10. Wang B, Niu Y, Miao L, et al. Decreased complexity in Alzheimer's disease: resting-State fMRI evidence of brain entropy mapping. *Front Aging Neurosci*. 2017;9:378. doi:10.3389/fnagi.2017.00378
11. Niu Y, Wang B, Zhou M, et al. Dynamic complexity of spontaneous BOLD activity in Alzheimer's disease and mild cognitive impairment using multiscale entropy analysis. *Front Neurosci*. 2018;12:677. doi:10.3389/fnins.2018.00677
12. Wang Z, AsDN Initiative, Brain entropy mapping in healthy aging and Alzheimer's disease. *Front Aging Neurosci*. 2020;12:596122. doi:10.3389/fnagi.2020.596122
13. Jann K, Boudreau J, Albrecht D, et al. FMRI complexity correlates with Tau-PET and cognitive decline in late-onset and autosomal dominant Alzheimer's disease. *J Alzheimers Dis*. 2023;95(2):437-451. doi:10.3233/JAD-220851
14. Zheng H, Onoda K, Nagai A, Yamaguchi S, Reduced dynamic complexity of BOLD signals differentiates mild cognitive impairment from normal aging. *Front Aging Neurosci*. 2020;12:90. doi:10.3389/fnagi.2020.00090
15. Maxim V, Sendur L, Fadili J, et al. Fractional Gaussian noise, functional MRI and Alzheimer's disease. *Neuroimage*. 2005;25(1):141-158. doi:10.1016/j.neuroimage.2004.10.044
16. Liu CY, Krishnan AP, Yan L, et al. Complexity and synchronicity of resting state blood oxygenation level-dependent (BOLD) functional MRI in normal aging and cognitive decline. *J Magn Reson Imaging*. 2013;38(1):36-45. doi:10.1002/jmri.23961
17. Grieder M, Wang DJJ, Dierks T, Wahlund LO, Jann K. Default mode network complexity and cognitive decline in mild Alzheimer's disease. *Front Neurosci*. 2018;12:770. doi:10.3389/fnins.2018.00770
18. Long Z, Jing B, Guo R, et al. A Brainnetome Atlas Based Mild Cognitive Impairment identification using hurst exponent. *Front Aging Neurosci*. 2018;10:103. doi:10.3389/fnagi.2018.00103
19. Ma X, Zhuo Z, Wei L, et al. Altered temporal organization of brief spontaneous brain activities in patients with Alzheimer's disease. *Neuroscience*. 2020;425:1-11. doi:10.1016/j.neuroscience.2019.11.025
20. Ren P, Ma M, Xie G, Wu Z, Wu D, AsDN Initiative. Altered complexity of resting-state BOLD activity in Alzheimer's disease-related neurodegeneration: a multiscale entropy analysis. *Aging (Albany NY)*. 2020;12(13):13571-13582. doi:10.18632/aging.103463
21. Costa M, Goldberger AL, Peng CK. Multiscale entropy analysis of complex physiologic time series. *Phys Rev Lett*. 2002;89(6):068102. doi:10.1103/PhysRevLett.89.068102
22. Wang DJJ, Jann K, Fan C, et al. Neurophysiological basis of multiscale entropy of brain complexity and its relationship with functional connectivity. *Front Neurosci*. 2018;12:352. doi:10.3389/fnins.2018.00352
23. Whitfield-Gabrieli S, Nieto-Castanon A. Conn: a functional connectivity toolbox for correlated and anticorrelated brain networks. *Brain Connect*. 2012;2(3):125-141. doi:10.1089/brain.2012.0073
24. Roediger DJ, Butts J, Falke C, et al. Optimizing the measurement of sample entropy in resting-state fMRI data. *Front Neurol*. 2024;15:1331365. doi:10.3389/fneur.2024.1331365
25. Yang AC, Tsai SJ, Lin CP, Peng CK. A Strategy to reduce bias of entropy estimates in resting-state fMRI signals. *Front Neurosci*. 2018;12:398. doi:10.3389/fnins.2018.00398
26. Desikan RS, Ségonne F, Fischl B, et al. An automated labeling system for subdividing the human cerebral cortex on MRI scans into gyral based regions of interest. *Neuroimage*. 2006;31(3):968-980. doi:10.1016/j.neuroimage.2006.01.021
27. Benjamini Y, Hochberg Y. Controlling the false discovery rate: a practical and powerful approach to multiple testing. *J R Stat Soc Series B (Methodol)*. 1995;57(1):12.
28. Jack CR, Bennett DA, Blennow K, et al. A/T/N: an unbiased descriptive classification scheme for Alzheimer disease biomarkers. *Neurology*. 2016;87(5):539-547. doi:10.1212/WNL.0000000000002923
29. Liu Y, Tan L, Wang HF, et al. Multiple effect of APOE genotype on clinical and neuroimaging biomarkers across Alzheimer's disease spectrum. *Mol Neurobiol*. 2016;53(7):4539-4547. doi:10.1007/s12035-015-9388-9397
30. Vannini P, Almkvist O, Dierks T, Lehmann C, Wahlund LO. Reduced neuronal efficacy in progressive mild cognitive impairment: a prospective fMRI study on visuospatial processing. *Psychiatry Res*. 2007;156(1):43-57. doi:10.1016/j.pscychresns.2007.02.003
31. Prvulovic D, Hubl D, Sack AT, et al. Functional imaging of visuospatial processing in Alzheimer's disease. *Neuroimage*. 2002;17(3):1403-1414. doi:10.1006/nimg.2002.1271
32. Terry DP, Sabatinelli D, Puente AN, Lazar NA, Miller LS. A meta-analysis of fMRI activation differences during episodic memory in Alzheimer's disease and mild cognitive impairment. *J Neuroimaging*. 2015;25(6):849-860. doi:10.1111/jon.12266
33. Malotaux V, Dricot L, Quenon L, Lhommel R, Ivanoiu A, Hanseeuw B. Default-mode network connectivity changes during the progression toward Alzheimer's dementia: a longitudinal functional magnetic resonance imaging study. *Brain Connect*. 2023;13(5):287-296. doi:10.1089/brain.2022.0008
34. Schultz AP, Buckley RF, Hampton OL, et al. Longitudinal degradation of the default/salience network axis in symptomatic individuals with elevated amyloid burden. *Neuroimage Clin*. 2020;26:102052. doi:10.1016/j.nicl.2019.102052
35. Kirova AM, Bays RB, Lagalwar S. Working memory and executive function decline across normal aging, mild cognitive impairment, and Alzheimer's disease. *Biomed Res Int*. 2015:748212. doi:10.1155/2015/748212
36. Wu SZ, Masurkar AV, Balcer LJ, Afferent and Efferent visual markers of Alzheimer's disease: a review and update in early stage disease. *Front Aging Neurosci*. 2020;12:572337. doi:10.3389/fnagi.2020.572337
37. Sun J, Wang B, Niu Y, et al. Complexity analysis of EEG, MEG, and fMRI in Mild Cognitive Impairment and Alzheimer's Disease: a review. *Entropy (Basel)*. 2020;22(2):239. doi:10.3390/e22020239
38. Sokunbi MO, Cameron GG, Ahearn TS, Murray AD, Staff RT. Fuzzy approximate entropy analysis of resting state fMRI signal complexity across the adult life span. *Med Eng Phys*. 2015;37(11):1082-1090. doi:10.1016/j.medengphy.2015.09.001
39. Dong J, Jing B, Ma X, Liu H, Mo X, Li H. Hurst exponent analysis of resting-state fMRI signal complexity across the adult lifespan. *Front Neurosci*. 2018;12:34. doi:10.3389/fnins.2018.00034
40. Smith RX, Yan L, Wang DJ. Multiple time scale complexity analysis of resting state FMRI. *Brain Imaging Behav*. 2014;8(2):284-291. doi:10.1007/s11682-013-9276-6
41. Jann K, Cen S, Santos M, et al. Effect of genetic risk on the relationship between rs-fMRI complexity and tau and amyloid PET in Alzheimer's disease. *J Alzheimers Dis*. 2024;101(2):429-435. doi:10.3233/JAD-240459

SUPPORTING INFORMATION

Additional supporting information can be found online in the Supporting Information section at the end of this article.

How to cite this article: Zhang R, Aksman L, Wijesinghe D, et al. A longitudinal study of functional brain complexity in progressive Alzheimer's disease. *Alzheimer's Dement*. 2025;17:e70059. https://doi.org/10.1002/dad2.70059